Analytic approach for the number statistics of non-Hermitian random matrices

Isaac Pérez Castillo,[1] Edgar Guzmán-González,[1] Antonio Tonatiúh Ramos Sánchez,[2] and Fernando L. Metz[3,4]
[1]*Departamento de Física, Universidad Autónoma Metropolitana-Iztapalapa, San Rafael Atlixco 186, Ciudad de México 09340, Mexico*
[2]*Instituto de Ciencias Nucleares, Universidad Nacional Autónoma de México, Cd. de México C.P. 04510, Mexico*
[3]*Physics Institute, Federal University of Rio Grande do Sul, 91501-970 Porto Alegre, Brazil*
[4]*London Mathematical Laboratory, 18 Margravine Gardens, London W6 8RH, United Kingdom*

(Received 28 July 2020; revised 15 April 2021; accepted 18 May 2021; published 2 June 2021)

We introduce a powerful analytic method to study the statistics of the number $\mathcal{N}_A(\gamma)$ of eigenvalues inside any smooth Jordan curve $\gamma \in \mathbb{C}$ for infinitely large non-Hermitian random matrices $\boldsymbol{A}$. Our generic approach can be applied to different random matrix ensembles of a mean-field type, even when the analytic expression for the joint distribution of eigenvalues is not known. We illustrate the method on the adjacency matrices of weighted random graphs with asymmetric couplings, for which standard random-matrix tools are inapplicable, and obtain explicit results for the diluted real Ginibre ensemble. The main outcome is an effective theory that determines the cumulant generating function of $\mathcal{N}_A$ via a path integral along γ, with the path probability distribution following from the numerical solution of a nonlinear self-consistent equation. We derive expressions for the mean and the variance of $\mathcal{N}_A$ as well as for the rate function governing rare fluctuations of $\mathcal{N}_A(\gamma)$. All theoretical results are compared with direct diagonalization of finite random matrices, exhibiting an excellent agreement.

DOI: 10.1103/PhysRevE.103.062108

I. INTRODUCTION

Since the pioneering work of Wigner [1], the study of random matrices has grown into a mature research area, with remarkable applications in physics, mathematics, biology, statistics, and finance [2,3]. This general character stems mainly from the versatility of random matrix ensembles, which can be thought of as simple but nontrivial models of strongly correlated systems.

The derivation of the joint probability distribution of eigenvalues (JPDE) is one of the most important successes of random matrix theory [4], since spectral observables defined in terms of the eigenvalues, including the spectral density and correlation functions [2], can be computed directly from the JPDE. For non-Hermitian random matrices with Gaussian distributed elements, Ginibre deduced the JPDE for matrices with complex and real quaternion entries [5]. Due to its simple form, the JPDE for the complex Ginibre case can be mapped in the Boltzmann distribution characterizing an electrostatic system of interacting charges [5]. This electrostatic analogy is at the core of the celebrated Dyson's Coulomb fluid approach [6], where the spectral observables follow from the partition function of an analogous physical system. The situation is considerable more difficult in the Ginibre ensemble with real matrix elements, owing to the existence of a finite fraction of real eigenvalues. In fact, the JPDE for the real Ginibre ensemble was derived only more than 25 years after Ginibre's paper in a breakthrough work by Lehmann and Sommers [7] (see also [8,9]). In this case, the electrostatic analogy becomes more complicated, as some image charges have to be incorporated and the eigenvectors couple to the eigenvalues in a nontrivial way (see [6,10] for further details).

Among several spectral observables that one may study in random matrix theory, one of particular importance with several applications is the distribution of the number $\mathcal{N}_D$ of eigenvalues contained in a certain domain D delimited by a smooth Jordan curve, the so-called *number statistics* or *full counting statistics* [2]. The study of the fluctuations of $\mathcal{N}_D$ is a rich mathematical problem on itself, and, likewise, many problems are transformed into the task of counting how many eigenvalues of a random matrix lie in a certain domain. Examples in this context are the study of the ground state of noninteracting fermions in a harmonic trap [11–15], the number of stable directions around the stationary points of disordered energy landscapes [16–18], the number of relevant fluctuation modes in principal component analysis [19–21], the localized or extended nature of eigenstates in disordered quantum systems [22–24], and the stability of large interacting biological systems [25,26], such as neural networks [27,28] and ecosystems [29–31].

Due to the well-developed machinery of the Coulomb fluid method, a complete picture of the typical and rare fluctuations of $\mathcal{N}_D$ has emerged for Gaussian *Hermitian* random matrices with complex, real, and real quaternion entries [11–13,18]. For non-Hermitian random matrices, the question of how many eigenvalues lie outside a disk in the complex plane has been addressed in the case of the real Ginibre ensemble [32]. However, the number statistics has been fully studied only for the complex Ginibre ensemble [14,15], for which there is a simple electrostatic analogy for the JPDE, and, consequently, the Coulomb fluid method is readily applied. Concerning the shape of D, Refs. [14,15] consider circular domains D, while results for noncircular domains have also been obtained by establishing a relation between the Ginibre ensemble and the

zeros of Gaussian analytic functions [33–35]. In contrast, results for non-Hermitian diluted matrices are scarce, and more complicated noncircular domains are mathematically out of reach in this case.

Ironically, non-Hermitian random matrices with *real* entries are very relevant for applications, especially in the study of high-dimensional nonequilibrium systems [25,27–31,36,37], where the matrix entries model the pairwise interactions between the system constituents [38]. Although in certain cases it is possible to compute $\mathcal{N}_D$ in terms of Fredholm determinants or Pfaffians [3,6,39], there is no generic analytic method to tackle the number statistics of real asymmetric random matrices, particularly in the case of sparse matrices, and the fluctuations of $\mathcal{N}_D$ remain poorly characterized.

In this work we design an analytic approach to determine the fluctuations of the number $\mathcal{N}_D$ of eigenvalues inside a domain $D \subset \mathbb{C}$ of arbitrary shape. We show how the study of the number statistics can be formulated for arbitrary ensembles of infinitely large non-Hermitian random matrices, with real or complex elements, and without relying on the analytic knowledge of the JPDE. In order to exemplify our analytic method, we derive, using the replica method, explicit results for the statistics of $\mathcal{N}_D$ in the case of a diluted version of the real Ginibre ensemble, where we consider symmetric adjacency matrices of random graphs with asymmetric couplings, for which an analytic expression for the JPDE is not available. The main outcome is a set of effective equations, valid for infinitely large random matrices, which determine all the cumulants and the large deviation function controlling, respectively, the typical and rare fluctuations of $\mathcal{N}_D$. The exactness of our theoretical approach is fully supported by numerical results obtained from the direct diagonalization of finite random matrices.

Although the theory developed here can be used, in principle, to study any random-matrix ensemble, the success of its application depends on the details of the particular ensemble considered. The replica method, as discussed in Appendix B, can be applied to various ensembles, provided they are of a mean-field type [i.e., the coupling strengths in Eq. (13) are independent of the distance between the spinors]. Examples include the adjacency matrix of asymmetric Erdös-Rényi random graphs, the adjacency matrix of directed random graphs with arbitrary degree distributions [38], and non-Hermitian random matrices with Gaussian distributed elements [5]. In the latter case, we expect that finite-size corrections are needed in order to take into account the slow dependency of the number variance with respect to N [40]. The replica calculation, as presented in Appendix B, does not apply to non-Hermitian systems defined on finite dimensional lattices, such as the Hatano-Nelson model [41] and optical lattices with non-Hermitian disorder [42,43].

The paper is organized as follows. In the next section we explain how the cumulant generating function of $\mathcal{N}_D$ can be written in terms of the partition function of an analogous system. Section III introduces the ensemble of sparse random matrices with asymmetric couplings considered here and presents the effective theory for the cumulant generating function in this case. We show numerical results for the diluted real Ginibre ensemble in Sec. IV, and we conclude in the last section. The paper also includes three appendices that essentially explain how to calculate the cumulant generating function for the ensemble of Sec. III using the replica method.

II. THE ANALYTIC METHOD FOR THE NUMBER STATISTICS

Let $\lambda_1, \ldots, \lambda_N$ be the eigenvalues of an $N \times N$ non-Hermitian random matrix $\boldsymbol{A}$ drawn from a distribution $\mathcal{P}(\boldsymbol{A})$. The number of eigenvalues inside a domain $D \subset \mathbb{C}$ enclosed by a smooth Jordan curve $\gamma = \partial D$ is given by

$$\mathcal{N}_{\boldsymbol{A}}(\gamma) = N \int_D dx\, dy \rho_{\boldsymbol{A}}(x, y), \tag{1}$$

where $\rho_{\boldsymbol{A}}(x, y)$ is the density of eigenvalues around the point $z = x + iy$:

$$\rho_{\boldsymbol{A}}(x, y) = \frac{1}{N} \sum_{i=1}^{N} \delta(x - \mathrm{Re}\lambda_i)\delta(y - \mathrm{Im}\lambda_i). \tag{2}$$

In the limit $N \to \infty$, the statistics of $\mathcal{N}_{\boldsymbol{A}}(\gamma)$ is encoded in the cumulant generating function (CGF)

$$\mathcal{F}_\gamma(\mu) = -\lim_{N\to\infty} \frac{1}{N} \ln\langle e^{-\mu \mathcal{N}_{\boldsymbol{A}}(\gamma)}\rangle, \tag{3}$$

with $\langle \ldots \rangle$ denoting the ensemble average with the distribution $\mathcal{P}(\boldsymbol{A})$. The derivatives of the CGF with respect to μ determine the cumulants of $\mathcal{N}_{\boldsymbol{A}}(\gamma)$. In particular, the intensive mean $N\kappa_1 = \langle \mathcal{N}_{\boldsymbol{A}} \rangle$ and variance $N\kappa_2 = \langle \mathcal{N}_{\boldsymbol{A}}^2 \rangle - \langle \mathcal{N}_{\boldsymbol{A}} \rangle^2$ read

$$\kappa_1 = \left.\frac{\partial \mathcal{F}_\gamma(\mu)}{\partial \mu}\right|_{\mu=0}, \qquad \kappa_2 = -\left.\frac{\partial^2 \mathcal{F}_\gamma(\mu)}{\partial \mu^2}\right|_{\mu=0}. \tag{4}$$

The CGF also provides information about the atypically large fluctuations of $\mathcal{N}_{\boldsymbol{A}}$. In fact, the probability that $\mathcal{N}_{\boldsymbol{A}} = Nn$ $(0 \leqslant n \leqslant 1)$ decays, for $N \to \infty$, as

$$\mathrm{Prob}_\gamma[\mathcal{N}_{\boldsymbol{A}} = Nn] \asymp e^{-N\Phi_\gamma(n)}, \tag{5}$$

where the rate function $\Phi_\gamma(n)$ is determined by the Legendre-Fenchel transform of the CGF [44,45]

$$\Phi_\gamma(n) = -\inf_{\mu\in\mathbb{R}}[\mu n - \mathcal{F}_\gamma(\mu)]. \tag{6}$$

Thus, our goal is precisely to calculate the CGF, since it contains all information about the number statistics.

The first step is to understand how $\mathcal{N}_{\boldsymbol{A}}$ depends on $\boldsymbol{A}$, so that we can compute, in principle, the ensemble average in Eq. (3). We rewrite the density of eigenvalues as [46]

$$\rho_{\boldsymbol{A}}(x, y) = \frac{1}{N\pi} \partial_z \partial_{z^*} \ln\det[(z\boldsymbol{I}_N - \boldsymbol{A})(z\boldsymbol{I}_N - \boldsymbol{A})^\dagger], \tag{7}$$

where $\partial_z = \frac{1}{2}(\frac{\partial}{\partial x} - i\frac{\partial}{\partial y})$, $\partial_{z^*} = \frac{1}{2}(\frac{\partial}{\partial x} + i\frac{\partial}{\partial y})$, and $\boldsymbol{I}_N$ is the N-dimensional identity matrix. Inserting the above equation back in Eq. (1) and using the Stokes' theorem, we obtain

$$\mathcal{N}_{\boldsymbol{A}}(\gamma) = -\oint_\gamma \frac{dz}{2\pi i} \partial_z \ln Q_{\boldsymbol{A}}(z, z^*), \tag{8}$$

where

$$Q_{\boldsymbol{A}}(z, z^*) = \frac{1}{\det[(\boldsymbol{A} - z\boldsymbol{I}_N)(\boldsymbol{A} - z\boldsymbol{I}_N)^\dagger]}, \tag{9}$$

with $(\cdots)^*$ and $(\cdots)^\dagger$ denoting complex and Hermitian conjugation, respectively. The arbitrary contour γ of integration in Eq. (8) is traversed once along the counterclockwise direction. By discretizing γ through a countable set of points $z_1, \ldots, z_L$, with $z_{L+1} \equiv z_1$ and $z_{l+1} \equiv z_l + \Delta z_l$, we get the formal identity

$$\mathcal{N}_{\boldsymbol{A}}(\gamma) = -\frac{1}{2\pi i} \lim_{L\to\infty} \sum_{l=1}^{L} [\ln Q_{\boldsymbol{A}}(z_{l+1}, z_l^*) - \ln Q_{\boldsymbol{A}}(z_l, z_l^*)], \tag{10}$$

and the CGF, Eq. (3), assumes the form

$$\mathcal{F}_\gamma(\mu) = -\frac{1}{N} \ln \left\langle \prod_{l=1}^{L} [Q_{\boldsymbol{A}}(z_{l+1}, z_l^*)]^{n_+} [Q_{\boldsymbol{A}}(z_l, z_l^*)]^{n_-} \right\rangle, \tag{11}$$

where $n_\pm = \pm\frac{\mu}{2\pi i}$. The limits $N \to \infty$ and $L \to \infty$ are implicit in Eq. (11).

Although Eqs. (9) and (10) expose how $\mathcal{N}_{\boldsymbol{A}}$ depends on $\boldsymbol{A}$, the calculation of the ensemble average in Eq. (11), with $Q_{\boldsymbol{A}}$ in its current form, seems a hopeless task. Using Gaussian integrals, we will rewrite $Q_{\boldsymbol{A}}$ in a quadratic form, suitable to compute the average $\langle(\cdots)\rangle$ using methods of statistical physics. Let us introduce the $2N \times 2N$ block matrix

$$\boldsymbol{F}_\eta(z, z^*) = \begin{pmatrix} \eta \boldsymbol{I}_N & i(z\boldsymbol{I}_N - \boldsymbol{A}) \\ i(z\boldsymbol{I}_N - \boldsymbol{A})^\dagger & \eta \boldsymbol{I}_N \end{pmatrix}, \tag{12}$$

which is related to $Q_{\boldsymbol{A}}$ via $Q_{\boldsymbol{A}} = \lim_{\eta\to 0^+} (\det \boldsymbol{F}_\eta)^{-1}$. The regularizer $\eta > 0$ ensures that $\boldsymbol{F}_\eta$ has a positive Hermitian part, which enables us to represent $Q_{\boldsymbol{A}}$ as a Gaussian integral over the spinors $\boldsymbol{\psi}_i \in \mathbb{C}^2$ $(i = 1, \ldots, N)$

$$Q_{\boldsymbol{A}}(z, z^*) = \lim_{\eta\to 0^+} \int \left(\prod_{i=1}^{N} d\boldsymbol{\psi}_i \, d\boldsymbol{\psi}_i^\dagger \right) \times \exp\left(-\sum_{i=1}^{N} \boldsymbol{\psi}_i^\dagger \boldsymbol{M}_\eta(z, z^*) \boldsymbol{\psi}_i + i \sum_{ij=1}^{N} \boldsymbol{\psi}_i^\dagger \boldsymbol{B}_{ij} \boldsymbol{\psi}_j \right), \tag{13}$$

where we introduced the 2×2 matrices

$$\begin{aligned} \boldsymbol{M}_\eta(z, z^*) &= \eta \boldsymbol{I}_2 + i(z\boldsymbol{\sigma}_+ + z^*\boldsymbol{\sigma}_-), \\ \boldsymbol{B}_{ij} &= A_{ij}\boldsymbol{\sigma}_+ + A_{ij}^\dagger \boldsymbol{\sigma}_-, \end{aligned} \tag{14}$$

and the ladder operators

$$\boldsymbol{\sigma}_+ = \begin{pmatrix} 0 & 1 \\ 0 & 0 \end{pmatrix}, \qquad \boldsymbol{\sigma}_- = \begin{pmatrix} 0 & 0 \\ 1 & 0 \end{pmatrix}. \tag{15}$$

Equation (13) is analogous to the partition function of a system with N spinors placed on the sites of a graph and coupled through the 2×2 matrices $\{\boldsymbol{B}_{ij}\}_{i,j=1,\ldots,N}$, i.e., $\boldsymbol{B}_{ij}$ quantifies the strength of the pairwise interactions between $\boldsymbol{\psi}_i$ and $\boldsymbol{\psi}_j$. The graph structure and the distribution of $\{\boldsymbol{B}_{ij}\}_{i,j=1,\ldots,N}$ are determined by the specific properties of $\mathcal{P}(\boldsymbol{A})$.

The analogy of $Q_{\boldsymbol{A}}$ with a partition function suggests that standard tools of statistical physics can be employed to calculate the CGF. However, there is an additional problem: the presence of the complex-valued exponents $n_\pm = \pm\frac{\mu}{2\pi i}$ in Eq. (11) hampers any direct attempt to evaluate $\langle(\cdots)\rangle$. To overcome this difficulty, we invoke the main strategy of the replica method [47,48] and compute, first, the ensemble average in Eq. (11) considering $n_\pm \in \mathbb{N}^+$. After performing the limit $N \to \infty$, the resulting $\mathcal{F}_\gamma(n_\pm)$ for $n_\pm \in \mathbb{N}^+$ is analytically continued to its limiting value as $n_\pm \to \pm\frac{\mu}{2\pi i}$ (see Appendix B). Although we do not prove rigorously that we can do such analytic continuation, the final equations of the method are verified by exact numerical diagonalizations of a particular random-matrix ensemble (see Sec. IV). Note that the product over $z_1, \ldots, z_L$ and the presence of the exponents $n_\pm \in \mathbb{N}^+$ in Eq. (11) do not formally change the quadratic form appearing inside $\langle(\cdots)\rangle$, a feature that is independent of the non-Hermitian random-matrix ensemble under study. In fact, the derivation of Eq. (B8) in Appendix B is fully general, i.e., valid for any contour $\gamma \in \mathbb{C}$ and for arbitrary non-Hermitian random-matrix ensembles, but the success in computing the ensemble average $\langle(\cdots)\rangle$ in Eq. (B8) and obtaining final equations for the CGF using the replica approach will depend on the choice of $\mathcal{P}(\boldsymbol{A})$, as emphasized in the previous section.

III. APPLICATION OF THE METHOD TO SPARSE RANDOM MATRICES

In the first part of this section we define an ensemble of sparse random matrices with asymmetric coupling strengths. In the second part, we apply our method to this ensemble and derive a set of equations that determine the CGF. These results will be useful on the next section, where we present explicit results for a diluted real Ginibre ensemble.

A. Sparse random matrices with asymmetric weights

In this work we illustrate the theory on the adjacency matrix of random graphs with asymmetric couplings [38]. It is convenient to write the matrix elements as $A_{ij} = c_{ij}J_{ij}$, where $c_{ij} \in \{0, 1\}$, $c_{ij} = c_{ji}$, and $c_{ii} = 0$. The binary entries $\{c_{ij}\}_{i,j=1,\ldots,N}$ encode the graph structure and $\{J_{ij}\}_{i,j=1,\ldots,N}$ represents the asymmetric interaction strengths, i.e., J_{ij} weights the influence of site i on site j. The random variables $\{c_{ij}\}_{i,j=1,\ldots,N}$ are drawn from

$$p_c(\{c_{ij}\}) = \prod_{i<j} \left[\frac{c}{N} \delta_{c_{ij},1} + \left(1 - \frac{c}{N}\right) \delta_{c_{ij},0} \right], \tag{16}$$

where $c \in \mathbb{R}^+$ is independent of N. Equation (16) yields *sparse* random matrices $\boldsymbol{A}$ with an average number c of nonzero elements per row and column in the limit $N \to \infty$. The couplings $\{J_{ij}\}_{i,j=1,\ldots,N}$ are independent identically distributed random variables drawn from a distribution p_J. The real asymmetric matrix $\boldsymbol{A}$ corresponds to the adjacency matrix of a weighted random graph with directed edges [38], where the number of neighbors connected to each node follows a Poisson distribution with average c [38,49]. Directed random graphs are key models of networked systems, such as the Internet, neural networks, and food webs (see [50] and references therein). The analytic formula for the JPDE of $\boldsymbol{A}$ is not known for sparse random-matrix ensembles, which renders traditional tools of random matrix theory unsuitable to study the number statistics.

B. The effective problem for the cumulant generating function

In Appendix B we explain how one calculates the average $\langle(\cdots)\rangle$ for the random-matrix ensemble given by Eq. (16), takes the limit $N \to \infty$ through the solution of a saddle-point integral, and finally performs the replica limit $n_\pm \to \pm\frac{\mu}{2\pi i}$. The main outcome is an *effective theory* defined over the space of functions mapping each point z along the curve γ onto a pair of 2×2 matrices $(\boldsymbol{\Gamma}(z), \boldsymbol{R}(z))$. The CGF is determined from

$$\mathcal{F}_\gamma(\mu) = -\frac{c}{2} + \ln\left\langle e^{-\frac{\mu}{2\pi i}\oint_\gamma dz \mathrm{Tr}\left[\boldsymbol{\Gamma}^{-1}(z)\boldsymbol{R}(z)\right]}\right\rangle_{\{\boldsymbol{\Gamma},\boldsymbol{R}\}} + \frac{c}{2}\left\langle\left\langle e^{-\frac{\mu}{2\pi i}\oint_\gamma dz \mathrm{Tr}[\boldsymbol{G}(z)\boldsymbol{H}(z)]}\right\rangle_{\boldsymbol{J}}\right\rangle_{\{\boldsymbol{\Gamma},\boldsymbol{R}\},\{\boldsymbol{\Gamma}',\boldsymbol{R}'\}}, \tag{17}$$

where we defined the auxiliary 2×2 matrices at $z \in \gamma$

$$\begin{aligned}\boldsymbol{G}(z) &= \left[\boldsymbol{I}_2 + \boldsymbol{\Gamma}'(z)\boldsymbol{J}\boldsymbol{\Gamma}(z)\boldsymbol{J}^\dagger\right]^{-1},\\ \boldsymbol{H}(z) &= \boldsymbol{\Gamma}'(z)\boldsymbol{J}\boldsymbol{R}(z)\boldsymbol{J}^\dagger + \boldsymbol{R}'(z)\boldsymbol{J}\boldsymbol{\Gamma}(z)\boldsymbol{J}^\dagger.\end{aligned} \tag{18}$$

The symbol $\langle\ldots\rangle_{\boldsymbol{J}}$ stands for the average over

$$\boldsymbol{J} = J\boldsymbol{\sigma}_+ + J'\boldsymbol{\sigma}_-, \tag{19}$$

with the real-valued interaction strengths J and J' independently drawn from p_J. The brackets $\langle(\cdots)\rangle_{\{\boldsymbol{\Gamma},\boldsymbol{R}\}}$ denote the average over all possible paths $\{\boldsymbol{\Gamma},\boldsymbol{R}\}$ along the curve γ. For an arbitrary functional $S[\{\boldsymbol{\Gamma},\boldsymbol{R}\}]$, we have

$$\langle S[\{\boldsymbol{\Gamma},\boldsymbol{R}\}]\rangle_{\{\boldsymbol{\Gamma},\boldsymbol{R}\}} = \int d\{\boldsymbol{\Gamma},\boldsymbol{R}\} w[\{\boldsymbol{\Gamma},\boldsymbol{R}\}]\, S[\{\boldsymbol{\Gamma},\boldsymbol{R}\}], \tag{20}$$

where $w[\{\boldsymbol{\Gamma},\boldsymbol{R}\}]$ is the path probability. A single path $\{\boldsymbol{\Gamma},\boldsymbol{R}\}$ can be thought of as the limit $L\to\infty$ of a sequence $\{\boldsymbol{\Gamma}(z_l),\boldsymbol{R}(z_l)\}_{l=1,\ldots,L}$, with $z_l \in \gamma$, while the path integration measure formally reads $d\{\boldsymbol{\Gamma},\boldsymbol{R}\} = \lim_{L\to\infty}\prod_{l=1}^{L} d\boldsymbol{\Gamma}(z_l)d\boldsymbol{R}(z_l)$. The path probability distribution $w[\{\boldsymbol{\Gamma},\boldsymbol{R}\}]$ follows from the solution of the self-consistency equation

$$w[\{\boldsymbol{\Gamma},\boldsymbol{R}\}] = \frac{1}{\Lambda}\sum_{k=0}^{\infty}\frac{e^{-c}c^k}{k!}\int\left(\prod_{r=1}^{k} d\{\boldsymbol{R}_r,\boldsymbol{\Gamma}_r\} w[\{\boldsymbol{R}_r,\boldsymbol{\Gamma}_r\}]\right) \times e^{\mu W[\{\boldsymbol{\Gamma},\boldsymbol{R}\}]}\langle\delta_{(\mathrm{F})}(\boldsymbol{R}-\boldsymbol{\Pi}_k)\delta_{(\mathrm{F})}(\boldsymbol{\Gamma}-\boldsymbol{\chi}_k)\rangle_{\boldsymbol{J}_{1,\ldots,k}}, \tag{21}$$

where $\langle\ldots\rangle_{\boldsymbol{J}_{1,\ldots,k}}$ is the average over $\boldsymbol{J}_1,\ldots,\boldsymbol{J}_k$, $\delta_{(\mathrm{F})}$ represents the functional Dirac delta in the path space, and Λ ensures the normalization of $w[\{\boldsymbol{\Gamma},\boldsymbol{R}\}]$. We have also introduced the 2×2 matrices at $z\in\gamma$:

$$\begin{aligned}\boldsymbol{\chi}_k(z) &= \left[\boldsymbol{M}_\eta(z,z^\star) + \sum_{r=1}^{k}\boldsymbol{J}_r\boldsymbol{\Gamma}_r(z)\boldsymbol{J}_r^\dagger\right]^{-1},\\ \boldsymbol{\Pi}_k(z) &= -\boldsymbol{\chi}_k(z)\left[i\boldsymbol{\sigma}_+ + \sum_{r=1}^{k}\boldsymbol{J}_r\boldsymbol{R}_r(z)\boldsymbol{J}_r^\dagger\right]\boldsymbol{\chi}_k(z).\end{aligned}$$

The statistical contribution of each path in Eq. (21) is also weighted according to an exponential factor, controlled by

$$W[\{\boldsymbol{\Gamma},\boldsymbol{R}\}] = \oint_\gamma\frac{dz}{2\pi i}\mathrm{Tr}\left[\boldsymbol{\Gamma}^{-1}(z)\boldsymbol{R}(z)\right]. \tag{22}$$

Equation (21) must be solved in the limit $\eta\to 0^+$.

IV. NUMERICAL RESULTS FOR SPARSE RANDOM MATRICES

Equation (17) for the CGF, together with Eq. (21) for the path probability, form the main outcome of our work, from which one can study, in the limit $N\to\infty$, the statistics of $\mathcal{N}_A$ for an ensemble of asymmetric and sparse random matrices defined by Eq. (16). In general, Eq. (21) has no explicit solution, and therefore one has to resort to a population dynamics approach [51,52] to obtain numerical solutions for $w[\{\boldsymbol{\Gamma},\boldsymbol{R}\}]$. In this numerical procedure, we discretize a single path over γ through a finite set $\{\boldsymbol{\Gamma}(z_i),\boldsymbol{R}(z_i)\}_{i=1,\ldots,L}$ containing L two-dimensional random matrices that are sampled consistently with Eq. (21) via a Monte Carlo scheme. The discrete representation of $w[\{\boldsymbol{\Gamma},\boldsymbol{R}\}]$ as the joint distribution of $\{\boldsymbol{\Gamma}(z_i),\boldsymbol{R}(z_i)\}_{i=1,\ldots,L}$ does not factorize, because different points along γ are correlated through the randomness of the graph ensemble.

Let us present explicit results for the fluctuations of $\mathcal{N}_A$ and compare our effective theory for $N\to\infty$ with direct diagonalization of finite random matrices. The mean and the variance of $\mathcal{N}_A$ follow from Eqs. (4):

$$\kappa_1 = -\langle W[\{\boldsymbol{\Gamma},\boldsymbol{R}\}]\rangle_{\{\boldsymbol{\Gamma},\boldsymbol{R}\}} - \frac{c}{2}\left\langle\oint_\gamma\frac{dz}{2\pi i}\langle\mathrm{Tr}[\boldsymbol{G}(z)\boldsymbol{H}(z)]\rangle_{\boldsymbol{J}}\right\rangle_{\{\boldsymbol{\Gamma},\boldsymbol{R}\},\{\boldsymbol{\Gamma}',\boldsymbol{R}'\}}, \tag{23}$$

$$\kappa_2 = \left\langle(W[\{\boldsymbol{\Gamma},\boldsymbol{R}\}])^2\right\rangle_{\{\boldsymbol{\Gamma},\boldsymbol{R}\}} - \langle W[\{\boldsymbol{\Gamma},\boldsymbol{R}\}]\rangle^2_{\{\boldsymbol{\Gamma},\boldsymbol{R}\}} + \frac{c}{2}\left\langle\left\langle\left(\oint_\gamma\frac{dz}{2\pi i}\mathrm{Tr}[\boldsymbol{G}(z)\boldsymbol{H}(z)]\right)^2\right\rangle_{\boldsymbol{J}}\right\rangle_{\{\boldsymbol{\Gamma},\boldsymbol{R}\},\{\boldsymbol{\Gamma}',\boldsymbol{R}'\}}, \tag{24}$$

where the path probability $w[\{\boldsymbol{\Gamma},\boldsymbol{R}\}]$ appearing in κ_1 and κ_2 is calculated at $\mu=0$. Figure 1 depicts the first two cumulants as a function of the radius R defining a disk centered at $z=0$, for average connectivities $c=3$ and $c=10$, and a real Gaussian distribution p_J with zero mean and variance $1/c$; this corresponds to a diluted version of the real Ginibre ensemble. Each shaded region delimits the error involved in the numerical solution of Eq. (21) using the population dynamics algorithm (see Appendix C). Figure 1 compares our theoretical findings with results obtained from the exact numerical diagonalizations of $N\times N$ adjacency matrices $\boldsymbol{A}$ with different N. The diagonalization results for the second cumulant show a stronger dependence with the matrix dimension, but they approach the theoretical results for increasing N.

For small c, the first two cumulants converge to a finite value as $R\to 0^+$, due to the existence of a δ-peak in $\rho(x,y)$ at $z=0$ [53]. Thus, the theory allows us to calculate the average and the variance of the weights characterizing the δ-peak contributions to the eigenvalue distribution in the limit $N\to\infty$. For larger values of c, the δ-peak disappears and the first cumulant resembles the behavior $\kappa_1\propto R^2$ observed in the complex Ginibre ensemble [15]. For $R\simeq 0$, κ_1 is slightly bigger than R^2, and it approaches R^2 from above as c is increased. The behavior of the variance of $\mathcal{N}_A$ for the diluted Ginibre ensemble is even more different than in the complex Ginibre ensemble [14,15]. Since κ_2 is finite for $R>0$, the variance of $\mathcal{N}_A$ scales linearly with $N\gg 1$, akin to the weak repulsion between the eigenvalues of sparse random matrices

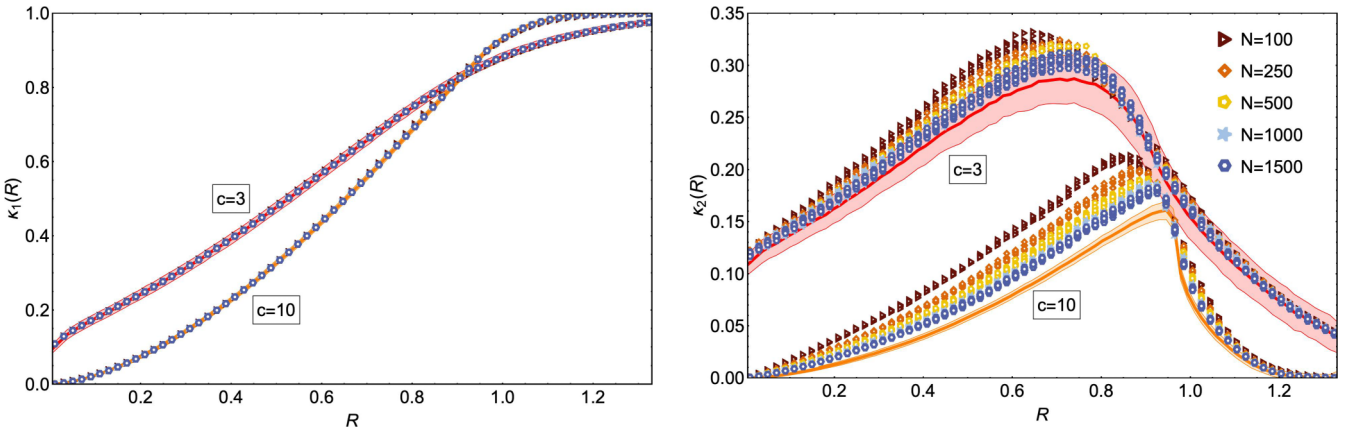

FIG. 1. The intensive mean κ_1 (left) and variance κ_2 (right) of the number of eigenvalues $\mathcal{N}_A$ within a disk of radius R centered at the origin of the complex plane. The random matrix $\boldsymbol{A}$ represents the adjacency matrix of random graphs [see Eq. (16)] with mean connectivities $c = 3$ (red solid line) and $c = 10$ (orange solid line). The asymmetric interactions are independently drawn from a Gaussian distribution p_J with zero mean and variance $1/c$. The theoretical solid lines are obtained from the solutions of Eqs. (23) and (24) using the population dynamics algorithm, while the markers are numerical diagonalization results of $N \times N$ random matrices. For the first cumulant we consider $N = 1500$, and for the second cumulant the values of N are indicated on the figure. The diagonalization results are averaged over 10^4 samples and the process is repeated 10 times, yielding the scatter plots shown in the figures; for the theoretical lines, the contour of the disk is discretized into 3000 points, and the population dynamics algorithm, employing a population size of 10^4, is iterated 4×10^7 times.

[52,54,55]. This scaling behavior is different from the complex Ginibre ensemble, where the dependence of the variance of $\mathcal{N}_A$ with the system size shows three remarkably different regimes [14,15]. The second cumulant, shown in Fig. 1, displays a nonmonotonic behavior with a maximum at a certain radius, whose location approaches $R = 1$ for increasing c, consistently with the sharp boundary of $\rho(x, y)$ in the dense limit $c \to \infty$ [15,53]. Besides the difference in the scaling of the variance of $\mathcal{N}_A$ with respect to N, the behavior of κ_2 in Fig. 1 is also different from the one of the complex Ginibre ensemble. In the latter case, the second cumulant is essentially a linear function of R in the interval $R \in [0, 1]$, and it decays rapidly to zero near $R = 1$ [15]. For the diluted Ginibre ensemble, we do not see such strong linear regime for different values of c up to $c = 10$. One can also notice that the error bars of κ_2 increase for lower values of c. This is because low values of c favor the appearance of isolated finite clusters in the corresponding random graph. The eigenvectors become localized on these finite clusters, which induces stronger fluctuations in the spectra, increasing the size of the error bars [56].

In Fig. 2 we present the theoretical results and the direct diagonalization results for the rate function $\Phi_\gamma(n)$ controlling the large deviations of the fraction $n = \frac{\mathcal{N}_A}{N}$ of eigenvalues inside a disk of radius $R = 0.5$. The shaded area in Fig. 2 bounds the error involved in the numerical solution of Eq. (21). The direct diagonalization results in Fig. 2 consistently approach the theoretical curve for increasing N, supporting the exactness of our theory. A striking property is the asymmetry of $\Phi_\gamma(n)$ around its minimum, located at $n = \kappa_1$. Sparse and asymmetric random matrices normally contain delocalized eigenvectors around $z = 0$ and localized eigenvectors close to the boundary of $\rho(x, y)$ [57,58]. Since the eigenvalue repulsion is stronger within the delocalized region [58], large fluctuations of n corresponding to an attraction of more eigenvalues to inside the disk are less likely, resulting in a rate function that grows faster for $n > \kappa_1$ in comparison to $n < \kappa_1$. This property is at variance with the Ginibre ensemble [15,32], whose rate function $\Phi_\gamma(n)$ is symmetric around its minimum due to the absence of localized eigenvectors.

V. CONCLUSIONS

While in the last decades there has been a leap forward in understanding the statistical properties related to the

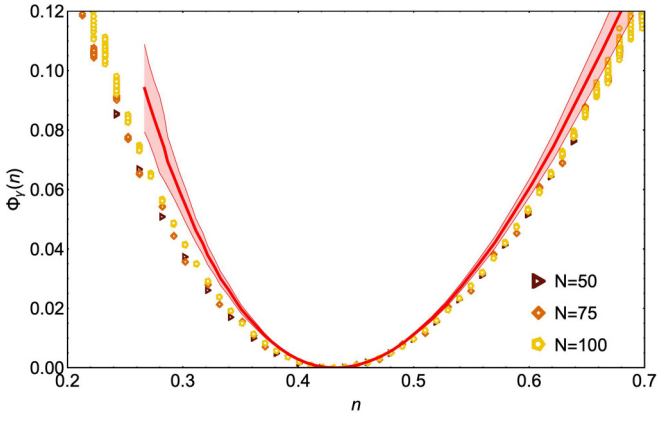

FIG. 2. Rate function $\Phi_\gamma(n)$ for the fraction n of eigenvalues of $\boldsymbol{A}$ inside a disk of radius 0.5 centered at the origin of the complex plane [see Eq. (5)]. The matrix $\boldsymbol{A}$ is the adjacency matrix of a random graph with mean connectivity $c = 4$ and asymmetric couplings drawn from a Gaussian distribution p_J with zero mean and variance $1/c$. The red solid line corresponds to our theoretical findings for $N \to \infty$, while the markers are the results of numerical diagonalizations of $N \times N$ random matrices. The diagonalization results are averaged over 10^7 samples and the process is repeated 10 times, yielding the scatter plots in the figure; for the theoretical line, the contour of the disk is discretized over 3000 points, and the population dynamics algorithm, with a population size of 10^4, is iterated 4×10^7 times.

spectrum of Hermitian random matrices, similar studies for non-Hermitian matrices, in particular those for sparse matrices, are still in their infancy. This is mostly due to a lack of mathematical tools to analyze systems with asymmetric interactions. In this paper we have developed a powerful technique to study the typical and atypical eigenvalue fluctuations of infinitely large non-Hermitian random matrices $\boldsymbol{A}$, and applied it to a diluted real Ginibre ensemble.

The method does not rely on the analytic knowledge of the joint probability distribution of eigenvalues, and it can be applied to various random-matrix ensembles of a mean-field type, where the random couplings in Eq. (13) do not depend on the distance between the sites. We have formulated the theory for arbitrary non-Hermitian random matrices [see Eq. (B8)], but we have applied the replica method and derived explicit results for an ensemble of weighted random graphs with asymmetric couplings [38]. The main outcome is an effective theory for the cumulant generating function of $\mathcal{N}_{\boldsymbol{A}}(\gamma)$, from which we computed the first two cumulants of $\mathcal{N}_{\boldsymbol{A}}$ and its large deviation behavior. In particular, we found that the large deviation probability of $\mathcal{N}_{\boldsymbol{A}}$ is asymmetric around its minimum, due to the existence of both delocalized and localized eigenvectors in the spectra of sparse asymmetric random matrices.

In the case of sparse random matrices, the variance of $\mathcal{N}_{\boldsymbol{A}}$ scales linearly with N, while $\langle \mathcal{N}_{\boldsymbol{A}}^2 \rangle - \langle \mathcal{N}_{\boldsymbol{A}} \rangle^2$ grows very slowly with N in the case of Gaussian random matrices. This fundamental difference has important consequences to the application of the replica method. Indeed, the scaling $\langle \mathcal{N}_{\boldsymbol{A}}^2 \rangle - \langle \mathcal{N}_{\boldsymbol{A}} \rangle^2 \propto \ln N$ observed in Gaussian Hermitian random matrices is recovered from the replica method when finite-size corrections are included in the saddle-point integral [40]. For Gaussian non-Hermitian random matrices, we expect that the situation is analogous, i.e., the results for the Ginibre ensemble [14,15] are reproduced from the formalism of Appendix B if finite-size fluctuations are taken into account in the solution of the saddle-point integral. This is an interesting open problem that we will consider in a future work.

The generality of our approach opens the door to investigate the fluctuations of other observables describing the spectra of directed random networks, such as the fraction of real eigenvalues, the index, and the spectral radius. All these quantities play an important role to characterize the stability of large biological systems [26,30–32].

ACKNOWLEDGMENTS

I.P.C., F.L.M., and E.G.-G. thank the London Mathematical Laboratory for financial support. F.L.M. also acknowledges a fellowship from CNPq/Brazil.

APPENDIX A: WRITING THE NUMBER OF EIGENVALUES OF A MATRIX INSIDE A CURVE AS A CONTOUR INTEGRAL

In this Appendix we present a method to obtain Eq. (8) for an arbitrary $N \times N$ non-Hermitian matrix $\boldsymbol{A}$. This approach is different from the one that is usually found in the literature.

Consider a region Ω of the complex plane enclosed by a smooth Jordan curve γ. Let $\lambda_1, \ldots, \lambda_N$ be the eigenvalues of $\boldsymbol{A}$, and define the function

$$E_{\boldsymbol{A}}(z, z^*) = \sum_{i=1}^{N} \frac{1}{z - \lambda_i}. \tag{A1}$$

By using the residue theorem, we perform the contour integral of $E_{\boldsymbol{A}}(z, z^*)$ and get the number of eigenvalues of $\boldsymbol{A}$ inside γ:

$$\mathcal{N}_{\boldsymbol{A}} = \oint_{\gamma} \frac{dz}{2\pi i} E_{\boldsymbol{A}}(z, z^*). \tag{A2}$$

Next, we find a nice expression for $E_{\boldsymbol{A}}(z, z^*)$. Consider the following function:

$$\varphi_{\boldsymbol{A}}(z, z^*) = \sum_{i=1}^{N} \ln[(z - \lambda_i)(z^* - \lambda_i^*)]. \tag{A3}$$

Clearly we have that $\partial_z \varphi_{\boldsymbol{A}}(z, z^*) = E_{\boldsymbol{A}}(z, z^*)$. Finally, note that $\varphi_{\boldsymbol{A}}(z, z^*) = -\ln Q_{\boldsymbol{A}}(z, z^*)$, where $Q_{\boldsymbol{A}}$ is given by (9). From here, Eq. (8) follows immediately.

APPENDIX B: COMPUTING THE CUMULANT GENERATING FUNCTION FOR RANDOM GRAPHS WITH ASYMMETRIC EDGES

In this Appendix we derive an expression for the *cumulant generating function* (CGF) of $\mathcal{N}_{\boldsymbol{A}}(\gamma)$ for the case of sparse random matrices $\boldsymbol{A}$ that correspond with the adjacency matrices of random graphs with asymmetric edges, as defined in the main text [see Eq. (16)]. First, we rewrite Eq. (8) in a more suitable form. We discretize the contour integral along γ by introducing a set of points $z_1, \ldots, z_L$ such that $z_{L+1} = z_1$ and $z_{l+1} = z_l + \Delta z_l$ for all l. Equations (8) and (3) can be reformulated as

$$\mathcal{N}_{\boldsymbol{A}}(\gamma) = -\frac{1}{2\pi i} \lim_{L\to\infty} \sum_{l=1}^{L} [\ln Q_{\boldsymbol{A}}(z_{l+1}, z_l^*) - \ln Q_{\boldsymbol{A}}(z_l, z_l^*)] \tag{B1}$$

and

$$\mathcal{F}_{\gamma}(\mu) = -\lim_{N\to\infty} \frac{1}{N} \lim_{L\to\infty} \lim_{n_{\pm}\to\pm\frac{\mu}{2\pi i}} \ln \left\langle \prod_{l=1}^{L} [Q_{\boldsymbol{A}}(z_{l+1}, z_l^*)]^{n_+} \times [Q_{\boldsymbol{A}}(z_l, z_l^*)]^{n_-} \right\rangle, \tag{B2}$$

respectively. Note that, in the previous equation, we commuted the ensemble average with the limit $L \to \infty$. Our final theoretical expressions are confirmed by direct diagonalization results (see Sec. IV), which strongly suggests that the above working hypothesis is valid. The next step is to express $Q_{\boldsymbol{A}}$ as a multivariate Gaussian integral. We first introduce the block matrix

$$\boldsymbol{F}_{\eta}(z, z^*) = \begin{pmatrix} \eta \boldsymbol{I}_N & i(z\boldsymbol{I}_N - \boldsymbol{A}) \\ i(z\boldsymbol{I}_N - \boldsymbol{A})^{\dagger} & \eta \boldsymbol{I}_N \end{pmatrix}, \tag{B3}$$

which is related to $Q_{\boldsymbol{A}}$ via $Q_{\boldsymbol{A}}(z, z^*) = \lim_{\eta\to 0^+} (\det \boldsymbol{F}_{\eta}(z, z^*))^{-1}$. The parameter $\eta > 0$ simply ensures that $\boldsymbol{F}_{\eta}$ has a positive Hermitian part, thus allowing us to represent $Q_{\boldsymbol{A}}$ as a multivariate Gaussian integral over a

set of spinors $\psi_i \in \mathbb{C}^2$, $i = 1, \ldots, N$,

$$Q_{\boldsymbol{A}}(z, z^*) = \lim_{\eta \to 0^+} \int \left[\prod_{i=1}^{N} \frac{d\psi_i \, d\psi_i^\dagger}{\pi^2} \right] e^{\mathcal{H}[\{\psi_i\}]}, \tag{B4}$$

with

$$\begin{aligned} \mathcal{H}[\{\psi_i\}] &= -\sum_{i=1}^{N} \psi_i^\dagger \boldsymbol{M}_\eta(z, z^*) \psi_i + i \sum_{i,j=1}^{N} \psi_i^\dagger \boldsymbol{B}_{ij} \psi_j, \\ \boldsymbol{M}_\eta(z, z^*) &= \eta \boldsymbol{I}_2 + i(z\boldsymbol{\sigma}_+ + z^* \boldsymbol{\sigma}_-), \\ \boldsymbol{B}_{ij} &= A_{ij} \boldsymbol{\sigma}_+ + A_{ij}^\dagger \boldsymbol{\sigma}_-, \end{aligned} \tag{B5}$$

and $\boldsymbol{\sigma}_+$, $\boldsymbol{\sigma}_-$ are the usual ladder operators

$$\boldsymbol{\sigma}_+ = \begin{pmatrix} 0 & 1 \\ 0 & 0 \end{pmatrix}, \qquad \boldsymbol{\sigma}_- = \begin{pmatrix} 0 & 0 \\ 1 & 0 \end{pmatrix}. \tag{B6}$$

Since $\psi_i = (u_i, v_i)^T$ is a spinor with components u_i, $v_i \in \mathbb{C}^2$, the measure $d\psi_i \, d\psi_i^\dagger$ is given by

$$\frac{d\psi_i \, d\psi_i^\dagger}{\pi^2} = \frac{d\mathrm{Re}u_i \, d\mathrm{Im}u_i}{\pi} \frac{d\mathrm{Re}v_i \, d\mathrm{Im}v_i}{\pi}. \tag{B7}$$

We will also write $d\Psi_i \equiv d\psi_i \, d\psi_i^\dagger / \pi^2$ in order to shorten the notation. Following the main strategy of the replica approach and assuming that $n_\pm$ are positive integers in Eq. (B2), we can rewrite this expression as follows:

$$\begin{aligned} e^{-N\mathcal{F}_\gamma(\mu)} = \int \left[\prod_{i=1}^{N} \prod_{l=1}^{L} \prod_{a=1}^{n_+} d\Psi_{i,la} \right] \left[\prod_{i=1}^{N} \prod_{l=1}^{L} \prod_{b=1}^{n_-} d\Phi_{i,lb} \right] \exp\left[-\sum_{i=1}^{N} \sum_{l=1}^{L} \left(\sum_{a=1}^{n_+} \psi_{i,la}^\dagger \boldsymbol{M}_\eta(z_{l+1}, z_l^*) \psi_{i,la} + \sum_{b=1}^{n_-} \phi_{i,lb}^\dagger \boldsymbol{M}_\eta(z_l, z_l^*) \phi_{i,lb} \right) \right] \\ \times \left\langle \exp\left[i \sum_{i<j}^{N} \sum_{l=1}^{L} \left\{ \sum_{a=1}^{n_+} \left(\psi_{i,la}^\dagger \boldsymbol{B}_{ij} \psi_{j,la} + \psi_{j,la}^\dagger \boldsymbol{B}_{ij}^\dagger \psi_{i,la} \right) + \sum_{b=1}^{n_-} \left(\phi_{i,lb}^\dagger \boldsymbol{B}_{ij} \phi_{j,lb} + \phi_{j,lb}^\dagger \boldsymbol{B}_{ij}^\dagger \phi_{i,lb} \right) \right\} \right] \right\rangle, \end{aligned} \tag{B8}$$

where, for simplicity, we have set $A_{ii} = 0$. We have also assumed that the limits appearing in Eq. (B2) are implicit. The next step is to calculate the average over the distribution of $\boldsymbol{A}$. Thus, we must consider a particular form for the ensemble of random matrices. Here we will present results for the adjacency matrix $\boldsymbol{A}$ of weighted Poisson graphs with asymmetric edges, where the matrix elements are defined as $A_{ij} = c_{ij} J_{ij}$, and $\{c_{ij}\}_{i,j=1,\ldots,N}$ are drawn from the distribution

$$p_c(\{c_{ij}\}) = \prod_{i<j} \left[\frac{c}{N} \delta_{c_{ij},1} + \left(1 - \frac{c}{N} \right) \delta_{c_{ij},0} \right],$$

with $c_{ij} = c_{ji}$ and $c_{ii} = 0$. The number of links connected to an arbitrary node follows a Poisson distribution with average $c \in \mathbb{R}^+$. The binary random variables $\{c_{ij}\}_{i,j=1,\ldots,N}$ tell who is connected to whom in the graph, while the real-valued variables $\{J_{ij}\}_{i,j=1,\ldots,N}$ control the strength of the pairwise interactions among different sites. These random variables are independently drawn from a distribution p_J, so that the weights of the directed links $i \to j$ and $j \to i$ are different, and the random matrix $\boldsymbol{A}$ is asymmetric. After carrying out the average over $\boldsymbol{A}$, we obtain the following expression for $N \gg 1$:

$$\begin{aligned} e^{-N\mathcal{F}_\gamma(\mu)} = \int \left[\prod_{i=1}^{N} \prod_{l=1}^{L} \prod_{a=1}^{n_+} d\Psi_{i,la} \right] \left[\prod_{i=1}^{N} \prod_{l=1}^{L} \prod_{b=1}^{n_-} d\Phi_{i,lb} \right] \exp\left[-\sum_{i=1}^{N} \sum_{l=1}^{L} \left(\sum_{a_l=1}^{n_+} \psi_{i,a_l}^\dagger \boldsymbol{M}_\eta(z_{l+1}, z_l^*) \psi_{i,a_l} + \sum_{b=1}^{n_-} \phi_{i,lb}^\dagger \boldsymbol{M}_\eta(z_l, z_l^*) \phi_{i,lb} \right) \right] \\ \times \exp\left[\frac{c}{2N} \sum_{i,j=1}^{N} \left\langle \exp\left[i \sum_{l=1}^{L} \left\{ \sum_{a=1}^{n_+} (\psi_{i,la}^\dagger \boldsymbol{J} \psi_{j,la} + \psi_{j,la}^\dagger \boldsymbol{J}^\dagger \psi_{i,la}) + \sum_{b=1}^{n_-} (\phi_{i,lb}^\dagger \boldsymbol{J} \phi_{j,lb} + \phi_{j,lb}^\dagger \boldsymbol{J}^\dagger \phi_{i,lb}) \right\} \right] - 1 \right\rangle_{\boldsymbol{J}} \right], \end{aligned} \tag{B9}$$

where $\langle (\cdots) \rangle_{\boldsymbol{J}}$ stands for the average over

$$\boldsymbol{J} = J\boldsymbol{\sigma}_+ + J'\boldsymbol{\sigma}_-, \tag{B10}$$

with the random interactions J and J' independently drawn from p_J.

Next, in order to decouple sites, we introduce the following order-parameter function:

$$P(\boldsymbol{\Psi}, \boldsymbol{\Phi}) = \frac{1}{N} \sum_{i=1}^{N} \prod_{l=1}^{L} \left[\prod_{a=1}^{n_+} \delta(\psi_{la} - \psi_{i,la}) \right] \left[\prod_{b=1}^{n_-} \delta(\phi_{lb} - \phi_{i,lb}) \right], \tag{B11}$$

with notation $P(\boldsymbol{\Psi}, \boldsymbol{\Phi}) \equiv P(\boldsymbol{\Psi}, \boldsymbol{\Phi}; \{\boldsymbol{\Psi}_i, \boldsymbol{\Phi}_i\}_{i=1}^N)$, and where we have introduced the shorthand notations $\boldsymbol{\Psi} = \{\psi_{la}\}$ and $\boldsymbol{\Phi} = \{\phi_{lb}\}$, for $l = 1, \ldots, L$, $a = 1, \ldots, n_+$, and $b = 1, \ldots, n_-$. Analogously, we have also defined $\boldsymbol{\Psi}_i \equiv \{\psi_{i,la}\}$ and $\boldsymbol{\Phi}_i \equiv \{\phi_{i,la}\}$, with $i = 1, \ldots, N$. After some tedious algebra, we can write $e^{-N\mathcal{F}_\gamma(\mu)}$ as the following path integral over $P(\boldsymbol{\Psi}, \boldsymbol{\Phi})$ and the conjugate order parameter $\hat{P}(\boldsymbol{\Psi}, \boldsymbol{\Phi})$,

$$e^{-N\mathcal{F}_\gamma(\mu)} = \int \mathcal{D}[\{P, \hat{P}\}] e^{-NS[\{P, \hat{P}\}]}, \tag{B12}$$

where $S[\{P,\hat{P}\}]$ is defined as follows:

$$S[\{P,\hat{P}\}] = -\ln\left\{\int d\boldsymbol{\Psi}\, d\boldsymbol{\Phi} \exp\left[-\sum_{l=1}^{L}\left(\sum_{a=1}^{n_+}\psi^{\dagger}_{a_l}\boldsymbol{M}(z_{l+1},z_l^*)\psi_{a_l} + \sum_{b=1}^{n_-}\phi^{\dagger}_{b_l}\boldsymbol{M}(z_l,z_l^*)\phi_{b_l}\right) - i\hat{P}(\boldsymbol{\Psi},\boldsymbol{\Phi})\right]\right\}$$
$$-\frac{c}{2}\int d\boldsymbol{\Psi}\, d\boldsymbol{\Psi}'\, d\boldsymbol{\Phi} d\boldsymbol{\Phi}' P(\boldsymbol{\Psi},\boldsymbol{\Phi})P(\boldsymbol{\Psi}',\boldsymbol{\Phi}')\left\langle e^{i\sum_{l=1}^{L}\left\{\sum_{a=1}^{n_+}[\psi^{\dagger}_{la}\boldsymbol{J}\psi'_{la}+(\psi'_{la})^{\dagger}\boldsymbol{J}^{\dagger}\psi_{la}]+\sum_{b=1}^{n_-}[\phi^{\dagger}_{lb}\boldsymbol{J}\phi'_{lb}+(\phi'_{lb})^{\dagger}\boldsymbol{J}^{\dagger}\phi_{lb}]\right\}} - 1\right\rangle_{\boldsymbol{J}}$$
$$-i\int d\boldsymbol{\Psi}\, d\boldsymbol{\Phi} P(\boldsymbol{\Psi},\boldsymbol{\Phi})\hat{P}(\boldsymbol{\Psi},\boldsymbol{\Phi}). \tag{B13}$$

1. The saddle-point method and the replica symmetric ansatz

Using the saddle-point method, the integral in Eq. (B12) is solved in the limit $N\to\infty$, resulting in $\int \mathcal{D}[\{P,\hat{P}\}]e^{-NS[\{P,\hat{P}\}]} \asymp e^{-NS[\{P_0,\hat{P}_0\}]}$, where $P_0, \hat{P}_0$ are a pair of functions that extremize the functional $S[\{P,\hat{P}\}]$. To be able to compute the limit $N\to\infty$, we assume that we can interchange the limit $N\to\infty$ with the limits $n\to 0, L\to\infty$, and $\eta\to 0$. We point out once more that the final outcome of our theory is independently confirmed by numerical diagonalization results, which strongly support the validity of such interchange of the order of limits.

Thus they obey the following saddle-point equations:

$$-i\hat{P}(\boldsymbol{\Psi},\boldsymbol{\Phi}) = c\int d\boldsymbol{\Psi}\, d\boldsymbol{\Phi} P(\boldsymbol{\Psi}',\boldsymbol{\Phi}')\left\langle e^{i\sum_{l=1}^{L}\{\sum_{a=1}^{n_+}[\psi^{\dagger}_{la}\boldsymbol{J}\psi'_{la}+(\psi'_{la})^{\dagger}\boldsymbol{J}^{\dagger}\psi_{la}]+\sum_{b=1}^{n_-}[\phi^{\dagger}_{lb}\boldsymbol{J}\phi'_{lb}+(\phi'_{lb})^{\dagger}\boldsymbol{J}^{\dagger}\phi_{lb}]\}} - 1\right\rangle_{\boldsymbol{J}}, \tag{B14}$$

$$P(\boldsymbol{\Psi},\boldsymbol{\Phi}) = \frac{\exp\left\{-\sum_{l=1}^{L}\left[\sum_{a=1}^{n_+}\psi^{\dagger}_{la}\boldsymbol{M}_{\eta}(z_{l+1},z_l^*)\psi_{la} + \sum_{b=1}^{n_-}\phi^{\dagger}_{lb}\boldsymbol{M}_{\eta}(z_l,z_l^*)\phi_{lb}\right] - i\hat{P}(\boldsymbol{\Psi},\boldsymbol{\Phi})\right\}}{\int d\boldsymbol{\Psi}' d\boldsymbol{\Phi}' \exp\left\{-\sum_{l=1}^{L}\left[\sum_{a=1}^{n_+}\psi'^{\dagger}_{la}\boldsymbol{M}_{\eta}(z_{l+1},z_l^*)\psi'_{la} + \sum_{b=1}^{n_-}\phi'^{\dagger}_{lb}\boldsymbol{M}_{\eta}(z_l,z_l^*)\phi'_{lb}\right] - i\hat{P}(\boldsymbol{\Psi}',\boldsymbol{\Phi}')\right\}}, \tag{B15}$$

where, for simplicity, we have dropped the subindex zero. To push further the derivation, we assume the replica symmetric (RS) ansatz

$$P(\boldsymbol{\Psi},\boldsymbol{\Phi}) = \int\left[\prod_{l=1}^{L} d\boldsymbol{\Sigma}_l\, d\boldsymbol{\Gamma}_l\right]\omega\left(\{\boldsymbol{\Sigma}_l,\boldsymbol{\Gamma}_l\}_{l=1}^{L}\right)\prod_{l=1}^{L}\left[\prod_{a=1}^{n_+}\frac{e^{-\psi^{\dagger}_{la}\boldsymbol{\Sigma}_l^{-1}\psi_{la}}}{\det\boldsymbol{\Sigma}_l}\prod_{b=1}^{n_-}\frac{e^{-\phi^{\dagger}_{lb}\boldsymbol{\Gamma}_l^{-1}\phi_{lb}}}{\det\boldsymbol{\Gamma}_l}\right], \tag{B16}$$

where $\boldsymbol{\Sigma}_l$ and $\boldsymbol{\Gamma}_l$ are 2×2 complex matrices defined for each $z_l\in\gamma$, and $\omega(\{\boldsymbol{\Sigma}_l,\boldsymbol{\Gamma}_l\}_{l=1}^{L})$ is the joint probability distribution of the pairs of matrices $\{\boldsymbol{\Sigma}_l,\boldsymbol{\Gamma}_l\}_{l=1}^{L}$ along the L points on the contour.

Combining Eqs. (B14) and (B15) in a single equation for $P(\boldsymbol{\Psi},\boldsymbol{\Phi})$, expanding its numerator in powers of c, using the RS ansatz (B16), and resolving the various integrals, we obtain the following self-consistency equation for $\omega(\{\boldsymbol{\Sigma}_l,\boldsymbol{\Gamma}_l\}_{l=1}^{L})$:

$$\omega\left(\{\boldsymbol{\Sigma}_l,\boldsymbol{\Gamma}_l\}_{l=1}^{L}\right) = \frac{1}{\Lambda}\sum_{k=0}^{\infty}\frac{e^{-c}c^k}{k!}\int\left[\prod_{r=1}^{k}dJ_r\prod_{l=1}^{L}d\boldsymbol{\Sigma}_{lr}\, d\boldsymbol{\Gamma}_{lr}\right]\left[\prod_{r=1}^{k}p_J(J_r)\omega\left(\{\boldsymbol{\Sigma}_{lr},\boldsymbol{\Gamma}_{lr}\}_{l=1}^{L}\right)\right]$$
$$\times\exp\left[-\frac{\mu}{2\pi i}\sum_{l=1}^{L}\ln\det\left(\boldsymbol{M}_{\eta}(z_{l+1},z_l^*)+\sum_{r=1}^{k}\boldsymbol{J}_r\boldsymbol{\Sigma}_{lr}\boldsymbol{J}_r^{\dagger}\right)+\frac{\mu}{2\pi i}\sum_{l=1}^{L}\ln\det\left(\boldsymbol{M}_{\eta}(z_l,z_l^*)+\sum_{r=1}^{k}\boldsymbol{J}_r\boldsymbol{\Gamma}_{lr}\boldsymbol{J}_r^{\dagger}\right)\right]$$
$$\times\prod_{l=1}^{L}\delta\left[\boldsymbol{\Sigma}_l-\frac{1}{\boldsymbol{M}_{\eta}(z_{l+1},z_l^*)+\sum_{r=1}^{k}\boldsymbol{J}_r\boldsymbol{\Sigma}_{lr}\boldsymbol{J}_r^{\dagger}}\right]\prod_{l=1}^{L}\delta\left[\boldsymbol{\Gamma}_l-\frac{1}{\boldsymbol{M}_{\eta}(z_l,z_l^*)+\sum_{r=1}^{k}\boldsymbol{J}_r\boldsymbol{\Gamma}_{lr}\boldsymbol{J}_r^{\dagger}}\right], \tag{B17}$$

where we have already performed the replica limit $n_{\pm}\to\pm\frac{\mu}{2\pi i}$, assuming that continuing the replica limit to imaginary values yields correct results. Similarly, we can also obtain an expression for the CGF by evaluating $S[\{P,\hat{P}\}]$, given by Eq. (B13), at the replica-symmetric saddle point. Inserting Eq. (B16) in Eq. (B13) and calculating the remainder integrals, we obtain

$$\mathcal{F}_{\gamma}(\mu) = -\ln\left\{\sum_{k=0}^{\infty}\frac{e^{-c}c^k}{k!}\int\left[\prod_{r=1}^{k}d\boldsymbol{J}_r p(J_r)\right]\left[\prod_{r=1}^{k}\prod_{l=1}^{L}d\boldsymbol{\Sigma}_{lr}d\boldsymbol{\Gamma}_{lr}\right]\prod_{r=1}^{k}\omega\left(\{\boldsymbol{\Sigma}_{lr},\boldsymbol{\Gamma}_{lr}\}_{l=1}^{L}\right)\right.$$
$$\left.\times\exp\left[-\frac{\mu}{2\pi i}\sum_{l=1}^{L}\ln\det\left(\boldsymbol{M}_{\eta}(z_{l+1},z_l^*)+\sum_{r=1}^{k}\boldsymbol{J}_r\boldsymbol{\Sigma}_{lr}\boldsymbol{J}_r^{\dagger}\right)+\frac{\mu}{2\pi i}\sum_{l=1}^{L}\ln\det\left(\boldsymbol{M}_{\eta}(z_l,z_l^*)+\sum_{r=1}^{k}\boldsymbol{J}_r\boldsymbol{\Gamma}_{lr}\boldsymbol{J}_r^{\dagger}\right)\right]\right\}$$

$$+\frac{c}{2}\int p_J(J)dJ\int\left[\prod_{l=1}^{L}d\boldsymbol{\Sigma}_l d\boldsymbol{\Gamma}_l\, d\boldsymbol{\Sigma}'_l\, d\boldsymbol{\Gamma}'_l\right]\omega\big(\{\boldsymbol{\Sigma}_l,\boldsymbol{\Gamma}_l\}_{l=1}^{L}\big)\omega\big(\{\boldsymbol{\Sigma}'_l,\boldsymbol{\Gamma}'_l\}_{l=1}^{L}\big)$$
$$\times\exp\left[-\frac{\mu}{2\pi i}\sum_{l=1}^{L}\ln\det\left(\boldsymbol{I}_2+\boldsymbol{\Sigma}_l\boldsymbol{J}\boldsymbol{\Sigma}'_l\boldsymbol{J}^\dagger\right)+\frac{\mu}{2\pi i}\sum_{l=1}^{L}\ln\det\left(\boldsymbol{I}_2+\boldsymbol{\Gamma}_l\boldsymbol{J}\boldsymbol{\Gamma}'_l\boldsymbol{J}^\dagger\right)\right]-\frac{c}{2}. \tag{B18}$$

The final step is to perform the continuous limit $L\to\infty$.

2. The continuous limit along the contour

Let us now take the continuous limit $L\to\infty$ in Eqs. (B17) and (B18). From the definition of $\boldsymbol{M}_\eta$, Eq. (B5), we obtain that

$$\boldsymbol{M}_\eta(z_{l+1},z_l^*)=\boldsymbol{M}_\eta(z_l,z_l^*)+i\Delta z_l\boldsymbol{\sigma}_+ +O\big(\Delta z_l^2\big), \tag{B19}$$

for $\Delta z_l\ll 1$. Henceforth we expand all quantities in powers of Δz_l up to the leading term. As a result, we get

$$\left[\boldsymbol{M}_\eta(z_{l+1},z_l^*)+\sum_{r=1}^{k}\boldsymbol{J}_r\boldsymbol{\Sigma}_{lr}\boldsymbol{J}_r^\dagger\right]^{-1}=\frac{1}{\boldsymbol{M}_\eta(z_l,z_l^*)+\sum_{r=1}^{k}\boldsymbol{J}_r\boldsymbol{\Sigma}_{lr}\boldsymbol{J}_r^\dagger}\left(\boldsymbol{I}_2-\sigma_+\frac{i\Delta z_l}{\boldsymbol{M}_\eta(z_l,z_l^*)+\sum_{r=1}^{k}\boldsymbol{J}_r\boldsymbol{\Sigma}_{lr}\boldsymbol{J}_r^\dagger}\right). \tag{B20}$$

From the arguments of the Dirac deltas appearing in the self-consistency, Eq. (B17), we see that it is convenient to make the following change of variables $\boldsymbol{\Sigma}_l=\boldsymbol{\Gamma}_l+\Delta z_l\boldsymbol{R}_l$, so that the r.h.s. of Eq. (B20) can be rewritten as

$$\boldsymbol{\Gamma}_l+\Delta z_l\boldsymbol{R}_l\leftarrow\frac{1}{\boldsymbol{M}_\eta(z_l,z_l^*)+\sum_{r=1}^{k}\boldsymbol{J}_r\boldsymbol{\Gamma}_{l,}\boldsymbol{J}_r^\dagger}+\Delta z_l\left[\frac{1}{\boldsymbol{M}_\eta(z_l,z_l^*)+\sum_{r=1}^{k}\boldsymbol{J}_r\boldsymbol{\Gamma}_{lr}\boldsymbol{J}_r^\dagger}i\sigma_+\frac{1}{\boldsymbol{M}_\eta(z_l,z_l^*)+\sum_{r=1}^{k}\boldsymbol{J}_r\boldsymbol{\Gamma}_{lr}\boldsymbol{J}_r^\dagger}\right.$$
$$\left.+\frac{1}{\boldsymbol{M}_\eta(z_l,z_l^*)+\sum_{r=1}^{k}\boldsymbol{J}_r\boldsymbol{\Gamma}_{lr}\boldsymbol{J}_r^\dagger}\sum_{r=1}^{k}\boldsymbol{J}_r\boldsymbol{R}_{lr}\boldsymbol{J}_r^\dagger\frac{1}{\boldsymbol{M}_\eta(z_l,z_l^*)+\sum_{r=1}^{k}\boldsymbol{J}_r\boldsymbol{\Gamma}_{lr}\boldsymbol{J}_r^\dagger}\right]. \tag{B21}$$

Plugging Eq. (B21) into Eqs. (B17) and (B18) and taking the continuous limit $L\to\infty$, we arrive at the final equations

$$\omega[\{\boldsymbol{R},\boldsymbol{\Gamma}\}]=\frac{1}{\Lambda}\sum_{k=0}^{\infty}\frac{e^{-c}c^k}{k!}\int\left[\prod_{r=1}^{k}d\{\boldsymbol{R}_r,\boldsymbol{\Gamma}_r\}\omega[\{\boldsymbol{R}_r,\boldsymbol{\Gamma}_r\}]\right]e^{\frac{\mu}{2\pi i}\oint_\gamma dz\mathrm{Tr}\left[\boldsymbol{R}(z)\boldsymbol{\Gamma}^{-1}(z)\right]}$$
$$\left\langle\delta_{(\mathrm{F})}\left[\boldsymbol{R}+\boldsymbol{\Gamma}\left(i\sigma_+ +\sum_{r=1}^{k}\boldsymbol{J}_r\boldsymbol{R}_r\boldsymbol{J}_r^\dagger\right)\boldsymbol{\Gamma}\right]\delta_{(\mathrm{F})}\left[\boldsymbol{\Gamma}-\frac{1}{\boldsymbol{M}_\eta+\sum_{r=1}^{k}\boldsymbol{J}_r\boldsymbol{\Gamma}_r\boldsymbol{J}_r^\dagger}\right]\right\rangle_{\boldsymbol{J}_{1,\ldots,k}} \tag{B22}$$

and

$$\mathcal{F}_\gamma(\mu)=\frac{c}{2}+\frac{c}{2}\int d\{\boldsymbol{R},\boldsymbol{\Gamma}\}d\{\boldsymbol{R}',\boldsymbol{\Gamma}'\}\omega[\{\boldsymbol{R},\boldsymbol{\Gamma}\}]\omega[\{\boldsymbol{R}',\boldsymbol{\Gamma}'\}]$$
$$\times\left\langle\exp\left(-\frac{\mu}{2\pi i}\oint_\gamma dz\mathrm{Tr}\left\{\left[\boldsymbol{I}_2+\boldsymbol{\Gamma}(z)\boldsymbol{J}\boldsymbol{\Gamma}'(z)\boldsymbol{J}^\dagger\right]^{-1}\left[\boldsymbol{R}(z)\boldsymbol{J}\boldsymbol{\Gamma}'(z)\boldsymbol{J}^\dagger+\boldsymbol{\Gamma}(z)\boldsymbol{J}\boldsymbol{R}'(z)\boldsymbol{J}^\dagger\right]\right\}\right)\right\rangle_{\boldsymbol{J}}$$
$$-\ln\left\langle\sum_{k=0}^{\infty}\frac{e^{-c}c^k}{k!}\int\left[\prod_{r=1}^{k}d\{\boldsymbol{R}_r,\boldsymbol{\Gamma}_r\}\omega[\{\boldsymbol{R}_r,\boldsymbol{\Gamma}_r\}]\right]\right.$$
$$\left.\times\exp\left\{-\frac{\mu}{2\pi i}\oint_\gamma dz\mathrm{Tr}\left[\left(\boldsymbol{M}_\eta(z)+\sum_{r=1}^{k}\boldsymbol{J}_r\boldsymbol{\Gamma}_r(z)\boldsymbol{J}_r^\dagger\right)^{-1}\left(i\sigma_+ +\sum_{r=1}^{k}\boldsymbol{J}_r\boldsymbol{R}_r(z)\boldsymbol{J}_r^\dagger\right)\right]\right\}\right\rangle_{\boldsymbol{J}_{1,\ldots,k}}, \tag{B23}$$

where $\langle\cdots\rangle_{\boldsymbol{J}_{1,\ldots,k}}$ denotes the average over the 2×2 matrices $\{\boldsymbol{J}_r\}_{r=1,\ldots,k}$ [see Eq. (B10)], $\delta_{(F)}$ represents the Dirac functional delta in the path space, and the path integration measure reads $d\{\boldsymbol{R},\boldsymbol{\Gamma}\}=\lim_{L\to\infty}\prod_{l=1}^{L}d\boldsymbol{R}(z_l)\,d\boldsymbol{\Gamma}(z_l)$. The above two equations are the main outcome of our work, since they determine the CGF of the random variable $\mathcal{N}_A(\gamma)$ in the limit $N\to\infty$.

APPENDIX C: POPULATION DYNAMICS ALGORITHM

In this Appendix we explain some aspects of the population dynamics algorithm. The key points of the algorithm can be found in [52,55], and here we discuss only those specific points that are different from previous works.

Notice that Eq. (B22) is a self-consistency equation for the functional probability density $\omega[\{\boldsymbol{R},\boldsymbol{\Gamma}\}]$ along the contour γ. Here $\omega[\{\boldsymbol{R},\boldsymbol{\Gamma}\}]$ corresponds to the path density for the pair of matrices $\boldsymbol{R}$ and $\boldsymbol{\Gamma}$ along γ, and therefore it contains all possible correlations of these matrices at any collection of points along γ. Since we are dealing with path integrals, solving

numerically Eq. (B22) seems a hopeless task. Fortunately, we can adapt the population dynamics algorithm to deal with this situation. The first step consists in discretizing the contour γ into a finite number of L points. It is important to realize that this discretization has nothing to do with the original discretization scheme we use to reach the aforementioned equations. Rather, we use a suitable discretization to resolve numerically the contour integrals appearing in the equations for $\omega[\{\boldsymbol{R}, \boldsymbol{\Gamma}\}]$ and $\mathcal{F}_\gamma(\mu)$ by seeking an integration algorithm that provides the most efficient quadratures along the contour γ. Thus, the functional density $\omega[\{\boldsymbol{R}, \boldsymbol{\Gamma}\}]$ is replaced by the joint distribution $\omega[\{\boldsymbol{R}(z_l), \boldsymbol{\Gamma}(z_l)\}_{l=1}^L]$. Then we proceed as usual, i.e., we introduce a population with a total number of M sets of matrices $\{\boldsymbol{R}_\alpha(z_1), \ldots, \boldsymbol{R}_\alpha(z_L), \boldsymbol{\Gamma}_\alpha(z_1), \ldots, \boldsymbol{\Gamma}_\alpha(z_L)\}_{\alpha=1}^M$ at each point $z_l \in \gamma$. The joint distribution $\omega[\{\boldsymbol{R}(z_l), \boldsymbol{\Gamma}(z_l)\}_{l=1}^L]$ is formally given by

$$\omega\big[\{\boldsymbol{R}(z_l), \boldsymbol{\Gamma}(z_l)\}_{l=1}^L\big] \sim \frac{1}{M}\sum_{\alpha=1}^{M}\prod_{l=1}^{L}\delta[\boldsymbol{R}(z_l) - \boldsymbol{R}_\alpha(z_l)]\delta[\boldsymbol{\Gamma}(z_l) - \boldsymbol{\Gamma}_\alpha(z_l)]. \tag{C1}$$

Then we use the standard weighted population dynamics algorithm to obtain a numerical solution of Eq. (B22). The original path probability density $\omega[\{\boldsymbol{R}, \boldsymbol{\Gamma}\}]$ is formally obtained from $\omega[\{\boldsymbol{R}(z_l), \boldsymbol{\Gamma}(z_l)\}_{l=1}^L]$ when $L \to \infty$ and $M \to \infty$.

[1] E. P. Wigner, Ann. Math. **67**, 325 (1958).
[2] M. L. Mehta, *Random Matrices*, Vol. 142 (Elsevier Science, Amsterdam, 2004).
[3] G. Akemann, J. Baik, and P. Di Francesco, *The Oxford Handbook of Random Matrix Theory*, Oxford Handbooks Online (Oxford University Press, New York, 2018).
[4] F. J. Dyson, J. Math. Phys. **3**, 1199 (1962).
[5] J. Ginibre, J. Math. Phys. **6**, 440 (1965).
[6] P. Forrester, *Log-Gases and Random Matrices*, London Mathematical Society Monographs Vol. 34 (Princeton University Press, Princeton, 2010).
[7] N. Lehmann and H.-J. Sommers, Phys. Rev. Lett. **67**, 941 (1991).
[8] A. Edelman, J. Multivariate Anal. **60**, 203 (1997).
[9] E. Kanzieper and G. Akemann, Phys. Rev. Lett. **95**, 230201 (2005).
[10] P. J. Forrester, Nucl. Phys. B **904**, 253 (2016).
[11] R. Marino, S. N. Majumdar, G. Schehr, and P. Vivo, Phys. Rev. Lett. **112**, 254101 (2014).
[12] I. Pérez Castillo, Phys. Rev. E **90**, 040102(R) (2014).
[13] R. Marino, S. N. Majumdar, G. Schehr, and P. Vivo, Phys. Rev. E **94**, 032115 (2016).
[14] B. Lacroix-A-Chez-Toine, S. N. Majumdar, and G. Schehr, Phys. Rev. A **99**, 021602(R) (2019).
[15] B. Lacroix-A-Chez-Toine, J. A. M. Garzón, C. S. H. Calva, I. Pérez Castillo, A. Kundu, S. N. Majumdar, and G. Schehr, Phys. Rev. E **100**, 012137 (2019).
[16] A. Cavagna, J. P. Garrahan, and I. Giardina, Phys. Rev. B **61**, 3960 (2000).
[17] D. Wales, R. Saykally, A. Zewail, and D. King, *Energy Landscapes: Applications to Clusters, Biomolecules and Glasses*, Cambridge Molecular Science (Cambridge University Press, Cambridge, 2003).
[18] S. N. Majumdar, C. Nadal, A. Scardicchio, and P. Vivo, Phys. Rev. Lett. **103**, 220603 (2009).
[19] S. N. Majumdar and M. Vergassola, Phys. Rev. Lett. **102**, 060601 (2009).
[20] E. Katzav and I. Pérez Castillo, Phys. Rev. E **82**, 040104(R) (2010).
[21] S. N. Majumdar and P. Vivo, Phys. Rev. Lett. **108**, 200601 (2012).
[22] A. D. Mirlin, Phys. Rep. **326**, 259 (2000).
[23] F. L. Metz and I. Pérez Castillo, Phys. Rev. B **96**, 064202 (2017).
[24] K. S. Tikhonov and A. D. Mirlin, Phys. Rev. B **99**, 024202 (2019).
[25] Y. V. Fyodorov and B. A. Khoruzhenko, Proc. Natl. Acad. Sci. USA **113**, 6827 (2016).
[26] F. L. Metz, I. Neri, and T. Rogers, J. Phys. A **52**, 434003 (2019).
[27] H. J. Sommers, A. Crisanti, H. Sompolinsky, and Y. Stein, Phys. Rev. Lett. **60**, 1895 (1988).
[28] K. Rajan and L. F. Abbott, Phys. Rev. Lett. **97**, 188104 (2006).
[29] R. M. May, Nature (London) **238**, 413 (1972).
[30] R. E. McMurtrie, J. Theor. Biol. **50**, 1 (1975).
[31] S. Allesina and S. Tang, Nature (London) **483**, 205 (2012).
[32] R. Allez, J. Touboul, and G. Wainrib, J. Phys. A **47**, 042001 (2014).
[33] M. Krishnapur and B. Virág, Int. Math. Res. Not. **2014**, 1441 (2014).
[34] S. Ghosh and A. Nishry, Comm. Pure Appl. Math. **72**, 3 (2019).
[35] S. Ghosh and M. Krishnapur, arXiv:1510.08814.
[36] H. Sompolinsky, A. Crisanti, and H. J. Sommers, Phys. Rev. Lett. **61**, 259 (1988).
[37] F. Schuessler, A. Dubreuil, F. Mastrogiuseppe, S. Ostojic, and O. Barak, Phys. Rev. Research **2**, 013111 (2020).
[38] M. Newman, *Networks: An Introduction* (Oxford University Press, Oxford, 2010).
[39] F. Bornemann, Markov Proc. Relat. Fields **16**, 803 (2010).
[40] F. L. Metz, J. Phys. A: Math. Theor. **50**, 495002 (2017).
[41] N. Hatano and D. R. Nelson, Phys. Rev. Lett. **77**, 570 (1996).
[42] A. F. Tzortzakakis, K. G. Makris, and E. N. Economou, Phys. Rev. B **101**, 014202 (2020).
[43] Y. Huang and B. I. Shklovskii, Phys. Rev. B **102**, 064212 (2020).
[44] H. Touchette, Phys. Rep. **478**, 1 (2009).
[45] A. Dembo and O. Zeitouni, *Large Deviations Techniques and Applications*, Vol. 38 (Springer, New York, 1998).
[46] J. Feinberg and A. Zee, Nucl. Phys. B **504**, 579 (1997).
[47] S. F. Edwards and P. W. Anderson, J. Phys. F **5**, 965 (1975).
[48] M. Mézard, G. Parisi, and M. Virasoro, *Spin Glass Theory and Beyond: An Introduction to the Replica Method and Its Applications*, Vol. 9 (World Scientific, Singapore, 1987).
[49] P. Erdős and A. Rényi, Publ. Math.-Debrecen **6**, 290 (1959).

[50] S. Bornholdt and H. Schuster, *Handbook of Graphs and Networks: From the Genome to the Internet* (Wiley, New York, 2006).
[51] M. Mézard and G. Parisi, Eur. Phys. J. B **20**, 217 (2001).
[52] F. L. Metz and I. Pérez Castillo, Phys. Rev. Lett. **117**, 104101 (2016).
[53] T. Rogers and I. Pérez Castillo, Phys. Rev. E **79**, 012101 (2009).
[54] F. L. Metz and D. A. Stariolo, Phys. Rev. E **92**, 042153 (2015).
[55] I. Pérez Castillo and F. L. Metz, Phys. Rev. E **97**, 032124 (2018).
[56] R. Kühn, J. Phys. A: Math. Theor. **41**, 295002 (2008).
[57] A. Amir, N. Hatano, and D. R. Nelson, Phys. Rev. E **93**, 042310 (2016).
[58] G. H. Zhang and D. R. Nelson, Phys. Rev. E **100**, 052315 (2019).